Impedance Matrix Analysis Technique in Wound Rotor Induction Machines Including General Rotor Asymmetry

Ahmad Salah and Youguang Guo
School of Electrical, Mechanical and Mechatronic Systems
University of Technology Sydney
Sydney, NSW 2007, Australia
Ahmad.a.salah@student.uts.au
Youguang.Guo-1@uts.edu.au

David Dorrell
Howard College Campus
University of KwaZulu Natal
Durban 4041, South Africa
Dorrelld@ukzn.ac.za

***Abstract*— A steady state analysis is developed for a wound rotor induction machine. In this paper the authors derive simple expressions for the mutual and coupling impedance in order to build impedance matrix. The analysis can be used in two ways when dealing with a symmetrical and asymmetrical rotor. The method is verified using an inverted-geometry wound motor; the analysis is then used to investigate an asymmetry fault on a 4 pole wound rotor. Experimental results (torque and current characteristic) are compared with computer predictions for the machine with both open-circuit and short-circuit faults.**

Keywords*— impedance matrix; squrrial cage induction machine (SCIM); wound rotor indctuion machine (WRIM)

I. INTRODUCTION

The wound rotor induction machine has enjoyed a renascence as the generator in many commercial wind turbines. It is used in a slip energy recovery manner so that it can generate both below and above the synchronous speed. In [1] and [2] many useful wound and cage rotor induction machine comparisons and explanations were put forward. However, there has been less work focused on wound rotor machine faults. The present paper is directed towards the development of a steady-state analysis of a wound rotor machine capable of including rotor asymmetry. Many papers in the past have stated methods for analyzing asymmetrical wound rotor machines based on simple positive and negative equivalent circuits for a machine with unbalanced impedance in the secondary circuit [3][4]. The analysis can be further extended to include additional rotor resistance and rotor voltages as would be found in a wound rotor softer starter (which is an old system) or a slip energy recovery scheme as found in the doubly-fed induction generator (DFIG) which is used in many wind turbine generators.

In order to evaluate rotor symmetry or asymmetry, it is first necessary to calculate the currents flowing in the various stator and rotor windings. This can be done using the coupling impedance method. Machine analysis breaks down the airgap flux density into a harmonic series of travelling waves with different pole numbers rotating in either direction [5]. These are derived from the currents and the spatial positioning of the stator and rotor conductors, which can finally be expressed in the form of a harmonic Fourier series of surface current density distributions. This leads to an expression for the conductor density distribution in terms of a harmonic series and can be obtained using complex Fourier analysis to account for the magnitude and positioning of conductors on the stator and rotor surfaces.

The harmonic conductor density method of analyzing machine windings has been used successfully in [5] and [6] to analyze cage induction machines with any number and distribution of bar and/or eccentricity faults. In [7] and [8], Williamson *et al.* used impedance matrices to detect the faults in cage rotor machines; however, the wound rotor machine works at a much higher slip than cage rotor machine, especially when used in a slip energy recovery scheme. The faults in these machines can vary greatly from their cage-rotor equivalent [9] and they are substantially higher. Here, the method was developed to include rotor coils groupings for wound rotor induction machine in the same way. The secondary part of wound rotor machines has a set of three-phase windings that are similar to those on the windings on the stator although the rotor slot number will vary and so will the rotor coil turn number. Thus, we can use the same method to find the rotor current and it will be more straightforward because the rotor loop currents do not share any common paths down bars. This method has several advantages, the main one being that any asymmetrical winding can be considered. In addition to this, the electric field in the airgap can be derived and the EMF induced into any winding calculated, leading to expressions for the coupling impedances between the various machine windings. These can be expressed in the form of an impedance matrix. The machine currents can be obtained from knowledge of the applied voltages when the matrix is solved. Thereafter it can be developed to incorporate eccentricity faults and also the condition monitoring of wound rotor machines, such as illustrated in [10] and [11]. The impedance matrix includes the impedances for the stator and rotor which are functions of the three-phase windings on the stator and rotor where

$$\begin{bmatrix} \bar{v}_s \\ 0 \\ 0 \\ 0 \\ 0 \end{bmatrix} = [\bar{Z}] \begin{bmatrix} \bar{I}_{s_f} \\ \bar{I}_{s_b} \\ \bar{I}^n_{r_1} \\ \bar{I}^n_{r_2} \\ \bar{I}^n_{r_3} \end{bmatrix} = \begin{bmatrix} \bar{Z}_{s,s_f} & 0 & \bar{Z}^n_{s_f,r_1} & \bar{Z}^n_{s_f,r_2} & \bar{Z}^n_{s_f,r_3} \\ 0 & \bar{Z}^n_{s,s_b} & \bar{Z}^n_{s_b,r_1} & \bar{Z}^n_{s_b,r_2} & \bar{Z}^n_{s_b,r_3} \\ \bar{Z}^n_{r_1,s_f} & \bar{Z}^n_{r_1,s_b} & \bar{Z}^n_{r_1,r_1} & \bar{Z}^n_{r_1,r_2} & \bar{Z}^n_{r_1,r_3} \\ \bar{Z}^n_{r_2,s_f} & \bar{Z}^n_{r_2,s_b} & \bar{Z}^n_{r_2,r_1} & \bar{Z}^n_{r_2,r_2} & \bar{Z}^n_{r_2,r_3} \\ \bar{Z}^n_{r_3,s_f} & \bar{Z}^n_{r_3,s_b} & \bar{Z}^n_{r_3,r_1} & \bar{Z}^n_{r_3,r_2} & \bar{Z}^n_{r_3,r_3} \end{bmatrix} \begin{bmatrix} \bar{I}_{s_f} \\ \bar{I}_{s_b} \\ \bar{I}^n_{r_1} \\ \bar{I}^n_{r_2} \\ \bar{I}^n_{r_3} \end{bmatrix} \quad (1)$$

This assumes the rotor to be short circuited.

When the rotor is symmetrical, that is before a fault occurs, there will be an MMF wave on the rotor rotating at slip frequency sf_m in the rotor coordinates. If there is asymmetry, then there will be a backwards rotating MMF wave. It subsequently induces EMFs of frequency $(1 - 2s)f_m$ in the stator windings. For that reason, it is necessary to add other components in the impedance matrix in order to accommodate the $(1 - 2s)f_m$ current components. The voltage is assumed to be zero for this component. At some stage in the 3-phase supply there will be star point that will short the path and additional source impedance for the f_m current can be added to the stator leakage impedance. The field which rotates forwards with respect to the rotor, and will be identified by the subscript f, will produce a field which rotates backwards with respect to the rotor when there is rotor asymmetry and will be identified by the subscript b. As the symmetry of the stator windings is maintained, the stator can be analyzed on a per phase basis.

The voltage vector is partitioned into stator and rotor terms. Assume the rotor windings are short circuited (no external impedances). Superscript (n) relates to stator harmonic; and s, r_1, r_2, and r_3 correspond to stator and rotor phase windings of the machine. $\bar{I}_{s_f}$ is the main input stator current and $\bar{I}_{s_b}$ the $(1 - 2s)$ times mains-frequency component.

II. Current Distribution in the Rotor of Squirrel Cage and Wound Rotor Induction Machine

When the rotor cage is symmetrical, the bar currents are of equal amplitude and the phase progression is fixed around the rotor periphery. The whole rotor cage current can then be represented by the current flowing in a single bar. It is clear that the rotor loop currents share common paths down bars. In Fig. 1(a), the number of current unknowns required to specify the rotor current distribution fully can be determined. If a cage has N_b bars, there will be $2N_b$ nodes and $3N_b$ branches. The currents [12] flow in loops comprising two adjacent rotor bars and the end-ring segments that join them, together with a circulating current I_e in one of the end rings if there is an end ring fault.

However, wound rotor has a complete set of three-phase windings that are similar to the windings on the stator, and the ends of the three rotor wires are connected to slip rings on the rotor shaft. They are usually permanently star connected on the rotor, otherwise 6 slip rings would be required not just 3. Thus we can get a similar expression for the 3-phase winding in the rotor. It will be more straightforward because the rotor loops currents (I_1, I_2 and I_3) do not share any common paths down bars, as shown in Fig. 1(b).

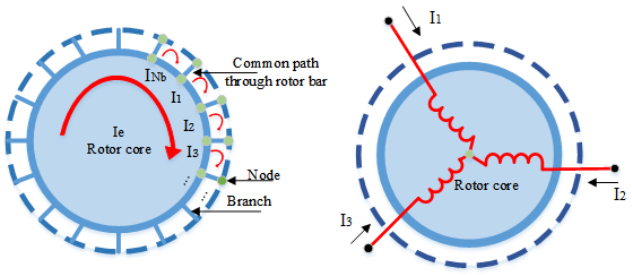

(a) (b)

Fig. 1. Current distribution in the cage and wound rotors. (a) Rotor cage, showing rotor-loop currents and the sharing common paths. (b) Wound Rotor, showing the three phase windings

III. Analysis of Impedance Matrix

The analysis will display the behavior of the wound rotor induction machine with balanced and unbalanced rotor windings. The following assumptions are made in this approach to determine coupling and mutual impedances for rotor and stator, assuming to simplify the analysis:

- Slotting effects are ignored so that the flux crosses the air-gap radially.
- The effect of saturation is ignored.

A. Fourier Analysis of the Machine-Winding

When a balanced three-phase voltage source supplies the stator winding, it produces a series of MMF harmonic distributions. The MMF distributions can be found by resolving the stator phase conductors into complex Fourier conductor density distribution. The technique was developed in [5] where the expression for the stator winding coefficient is defined by the spatial distribution of all the coils. The stator winding coefficient of one phase winding is

$$\bar{N}^n_{st} = \frac{k}{2\pi} \sum_{w=1}^{N_s} k_s C_w e^{jnp_m ky} \quad (2)$$

where N_s is the number of slots that the winding is located in, C_w is the number of series winding turns in a slot, and y is the spatial location of the slot. k is the inverse of the average gap radius. The slot opening factor is defined by the slot opening b_s so that

$$k_s = \frac{2\sin(0.5np_m kb_s)}{np_m kb_s} \quad (3)$$

If the 3-phase supply is balanced with series connected stator windings, the MMF wave is

$$j_{st}(y,t) = \mathrm{Re} \sum_{n=-\infty}^{\infty} \bar{J}^n_{st} e^{j(\omega t - np_m ky)} \quad (4)$$

where, for a balanced 3-phase current set, and using the identity $a = e^{(j2\pi/3)}$, the MMF magnitude is

$$\bar{J}^n_{st} = \bar{N}^n_{st}\left(1 + a^{1-n}a^{n-1} + a^{n-1}a^{1-n}\right)\bar{I}_s = 3\bar{N}^n_{st}\bar{I}_s \quad (5)$$

and the fundamental pole-pair number of the machine is p_m. This will include winding harmonics n.

The rotor conductor distribution is obtained in a similar manner to the stator phase windings. If (+C,-C) is a coil in the first phase winding in the rotor (r), Fig. 2, where x is the variation in the axial direction, and y' is the variation in the tangential direction. If this is represented as having finite conductor width b_r (the rotor slot opening), the conductor density over the slot opening is the number of coil turns divided by the slot opening. Its distribution can be represented as a complex Fourier series using the definitions in Fig. 2. The winding coefficient is defined by the spatial distribution of all the coils

$$\bar{N}_r^{\nu} = \frac{k}{2\pi}\sum_{w=1}^{N_R} k^{\nu}{}_r C_r e^{j\nu p_m k y'} \tag{6}$$

N_R is the total number of slots on rotor, and C_r is the effective rotor turns per phase. The slot opening factor is defined by the rotor slot opening b_r (in m) so that

$$k_r = \frac{2\sin(0.5np_m kb_r)}{np_m kb_r} \tag{7}$$

For a balanced three-phase rotor windings (r_1, r_2 and r_3), the ν^{th} harmonic conductor density distributions are given by

$$\begin{aligned} \bar{N}_{r_1}^{\nu} &= \bar{N}_r{}^{\nu} e^{-j\nu p_m k y'}, \\ \bar{N}_{r_2}^{\nu} &= a^{\nu}\bar{N}_r{}^{\nu} e^{-j\nu p_m k y'}, \\ \bar{N}_{r_3}^{\nu} &= a^{-\nu}\bar{N}_r{}^{\nu} e^{-j\nu p_m k y'} \end{aligned} \tag{8}$$

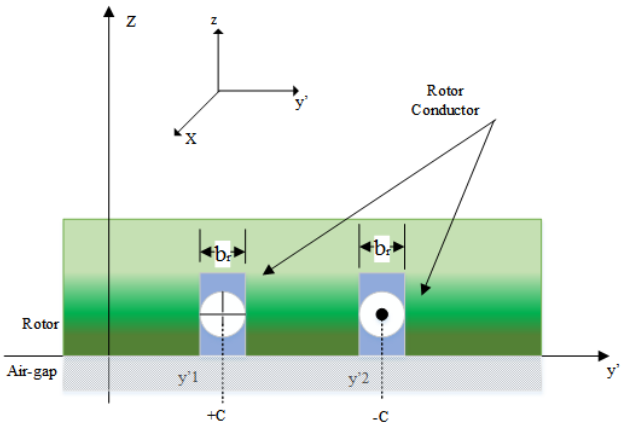

Fig. 2. Single coil (+C,-C) positioned on Rotor.

A particular n^{th} harmonic current in the rotor will in turn set up a complete series of ν^{th} harmonic distribution in the airgap, so that

$$J^{n\nu}{}_{r_1}(y',t) = \bar{I}_{r_1}^{n}\bar{N}_{r_1}^{\nu} e^{j(s_n\omega t - nky')} \tag{9}$$

B. Coupling and Mutual Impedances

The remainder of the section will be devoted to the determination of the impedances, then an extension of the impedance matrix to include external impedances and rotor voltages is put forward.

1) Stator-stator coupling impedance: The airgap field can be expressed using (5) and hence the back-EMF in the stator winding. This can then be related to the supply current, by the stator-stator coupling impedance. The stator impedance can be written with reference to the forward rotating fluxes and backward rotating fluxes where

$$\begin{aligned} \bar{Z}_{s,s_f} &= R_s + jX_s + jX_{ss} \\ \bar{Z}_{s,s_b} &= R_s + j(1-2s)\left(X_s + jX_{ss}\right) \end{aligned} \tag{10}$$

R_a and X_s are the stator resistance and leakage inductance. X_{ss} is the magnetizing reactance for the three-phase winding:

$$X_{ss} = 3\frac{2\pi\mu_0\omega L_{st}\bar{N}_{st}^{1}}{k^3 p_m^2 g}\left(\bar{N}_{st}^{1}\right)^{*} \tag{11}$$

2) Stator-rotor coupling impedance: Using (5) to provide an expression for air-gap field which produced by the stator winding:

$$b_{st}(x,y,t) = \text{Re}\sum_{n=-\infty}^{\infty}\left[\bar{B}_{st}^{n} e^{j(\omega t - np_m ky)}\right] \tag{12}$$

the field magnitudes are

$$\bar{B}_{st}^{n} = \frac{j\mu_0\bar{J}_{st}^{n}}{knp_m g} \tag{13}$$

Transferring to a rotor reference frame, it becomes

$$\bar{B}_{rt}^{n} = \text{Re}\sum_{n=-\infty}^{\infty}\left[\bar{B}_{st}^{n} e^{j(s\omega t - np_m ky')}\right] \tag{14}$$

Eq. (15) provides an expression for the stator-rotor coupling impedance, and it includes a conventional rotor skew factor k_{sk} which is obtained from (16) so that

$$\bar{Z}_{r_1,s_f} = 3\frac{j2\pi\mu_0\omega s L_{st} k_{sk}\bar{N}_{st}^{1}}{k^3 np_m^2 g}\left(\bar{N}_{r1}^{1}\right)^{*} \tag{15}$$

$$k_{sk} = \frac{\sin\left(np_m\theta_{sk}/2\right)}{\left(np_m\theta_{sk}/2\right)} \tag{16}$$

The coupling impedances for the other rotor phases can be related to $\bar{Z}_{r_1,s}$ as

$$\bar{Z}_{r_2,s_f} = a^{-n}\bar{Z}_{r_1,s_f} \text{ and } \bar{Z}_{r_3,s_f} = a^{n}\bar{Z}_{r_1,s_f} \tag{17}$$

The EMFs induced in the rotor windings by the stator airgap flux wave which rotates backwards with respect to the rotor are of equal amplitude, but the phase progression is reversed. Thus, we can get $\bar{Z}_{r,s_b}$ for the rotor phases.

3) Rotor-stator coupling impedance: The rotor phase windings will have currents at slip frequency, which is appropriate to the stator field which induces it. The current in the rotor will be obtained from (9) and referred to the stator reference frame

$$J^{n\nu}{}_{r_1}(y',t) = \bar{I}_{r_1}^{n}\bar{N}_{r_1}^{\nu} e^{j(s_f\omega t - nky)} \tag{18}$$

where $s_f = 1-(n-\nu)(1-s)$,
$n = 1, -5, 7, \ldots$, and $\nu = \pm 1, \pm 3 \pm 5, \ldots$

The rotor–stator coupling impedance is $\bar{Z}_{s,r_1}$, and s_f = 1 so that

$$\bar{Z}_{s_f,r_1} = \frac{j2\pi\mu_0\omega s_f L_{st} k_{sk} \bar{N}^1_{r_1}}{k^3 p_m^2 g}\left(\bar{N}^1_{st}\right)^* \tag{19}$$

$$\bar{Z}_{s_f,r_2} = a^n \bar{Z}_{s_f,r_1}, \bar{Z}_{s_f,r_3} = a^{-n}\bar{Z}_{s_f,r_1} \tag{20}$$

and $\bar{Z}_{s_b,r}$ is equal to $\bar{Z}_{s_f,r}$ but multiplied by s_b instead of s_f, where $s_b = s_f(2s-1)$.

4) Rotor-rotor coupling impedances: The rotor current produces a harmonic series distribution, which induce back-EMFs into the rotor. These induced voltages can be summed together to produce an impedance in the same way in stator winding

$$\bar{Z}^n_{r_1,r_1} = \bar{Z}^n_{r_2,r_2} = \bar{Z}^n_{r_3,r_3} = \frac{2}{3} j s_n \sum_m X_{rr} \tag{21}$$

X_{rr} represents the unreferred m^{th} harmonic rotor magnetizing reactance. And the factor (2/3) converts magnetizing reactance from a three phase winding to a single phase winding. The mutual coupling impedances between the rotor phases are determined from

$$\begin{aligned} \bar{Z}^n_{r_2,r_1} &= \bar{Z}^n_{r_3,r_2} = \frac{2}{3} j s_n \sum_m \cos(2\pi/3) X_{rr} \\ X_{rr} &= \frac{2\pi\mu_0\omega s_n L_{st} k_{sk} \bar{N}^1_r}{k^3 n p_m^2 g}\left(\bar{N}^1_r\right)^* \end{aligned} \tag{22}$$

The rotor self-impedances are also modified to include resistance and the leakage inductance so that

$$\bar{Z}^n_{r_1,r_1} = \bar{Z}^n_{r_2,r_2} = \bar{Z}^n_{r_3,r_3} = (R_r + j s_n X_r) + \frac{2}{3} j s_n X_{rr} \tag{23}$$

C. Voltage Equations

The impedance matrix can be reduced to the following simplified form, so we can get one equivalent circuit for fundamental wave and single rotor phase when the rotor has a balanced three phase set:

$$\begin{bmatrix} \bar{v}_s \\ 0 \end{bmatrix} = \begin{bmatrix} \bar{Z}^1_{s,s} & \bar{Z}^1_{s,r_1} \\ \bar{Z}^1_{r_1,s} & \bar{Z}^1_{r_1,r_1} \end{bmatrix} \begin{bmatrix} \bar{I}_s \\ \bar{I}_{r_1} \end{bmatrix} \tag{24}$$

Substituting for the impedance components and rearranging results in two voltage equations:

$$\begin{aligned} v_s &= \bar{Z}^1_{s,s}\bar{I}_s + \bar{Z}^1_{s,r_1}\bar{I}_{r_1} \\ 0 &= \bar{Z}^1_{r_1,s}\bar{I}_s + \bar{Z}^1_{r_1,r_1}\bar{I}_{r_1} \end{aligned} \tag{25}$$

D. Electromagnetic Torque

The impedance matrix is first assembled, and then modified to produce the desired fault condition. The power may be determined in a straightforward from the applied phase voltage and current. The electromagnetic torque that is developed by the machine can be determined from the current density distributions of the stator and rotor [7], which is produced as a result of the interaction between these two field components. The torque is given by

$$T = \frac{2\pi r^2 \mu_o L_{st}}{p_m g} \mathrm{Re}\left\{ \begin{aligned} &j\left(\bar{J}_{st_b}\bar{J}_{r_b}{}^* - \bar{J}_{st_f}\bar{J}_{r_f}{}^*\right) \\ &+ j\left(\bar{J}_{st_b}\bar{J}_{r_f} - \bar{J}_{st_f}\bar{J}_{r_b}\right)e^{j2s\omega t} \end{aligned} \right\} \tag{26}$$

in which steady and pulsating components may be identified.

The forwards components of the stator MMF were defined earlier and the backward components of the stator and rotor MMF are given as in [6]. So that

$$\bar{J}^n_{st_b} = \bar{N}^{n*}_{st}\left(1 + a^{1-n}a^{n-1} + a^{n-1}a^{1-n}\right)\bar{I}_s = 3\bar{N}^{n*}_{st}\bar{I}_s \tag{27}$$

$$\bar{J}_{r_b}{}^{n\nu}(y',t) = 3\bar{I}^n_r \bar{N}^{\nu *}_r e^{j(s_n\omega t - nky')} \tag{28}$$

E. Inclusion of Rotor external circuits

In order to consider any additional circuitry associated with non-supply frequency source impedance (stator winding), soft starting (extra rotor impedance), and slip energy recovery voltages from an inverter, then (1) can be further developed:

$$\begin{bmatrix} \bar{v}_s \\ 0 \\ \bar{v}_{r1} \\ \bar{v}_{r2} \\ \bar{v}_{r3} \end{bmatrix} = \begin{bmatrix} \bar{Z}_{s,s_f} & 0 & \bar{Z}^n_{s_f,r_1} & \bar{Z}^n_{s_f,r_2} & \bar{Z}^n_{s_f,r_3} \\ 0 & \bar{Z}^{n/}_{s,s_b} & \bar{Z}^n_{s_b,r_1} & \bar{Z}^n_{s_b,r_2} & \bar{Z}^n_{s_b,r_3} \\ \bar{Z}^n_{r_1,s_f} & \bar{Z}^n_{r_1,s_b} & \bar{Z}^{n/}_{r_1,r_1} & \bar{Z}^n_{r_1,r_2} & \bar{Z}^n_{r_1,r_3} \\ \bar{Z}^n_{r_2,s_f} & \bar{Z}^n_{r_2,s_b} & \bar{Z}^n_{r_2,r_1} & \bar{Z}^{n/}_{r_2,r_2} & \bar{Z}^n_{r_2,r_3} \\ \bar{Z}^n_{r_3,s_f} & \bar{Z}^n_{r_3,s_b} & \bar{Z}^n_{r_3,r_1} & \bar{Z}^n_{r_3,r_2} & \bar{Z}^{n/}_{r_3,r_3} \end{bmatrix} \begin{bmatrix} \bar{I}_{s_f} \\ \bar{I}_{s_b} \\ \bar{I}^n_{r_1} \\ \bar{I}^n_{r_2} \\ \bar{I}^n_{r_3} \end{bmatrix}$$

$$\text{where } \bar{Z}^{n/}_{s,s_b} = \bar{Z}^n_{s,s_b} + Z_{ex,S},\ \bar{Z}^{n/}_{r_1,r_1} = \bar{Z}^n_{r_1,r_1} + Z_{ex,r1} \tag{29}$$

$$\bar{Z}^{n/}_{r_2,r_2} = \bar{Z}^n_{r_2,r_2} + Z_{ex,r2}\text{, and } \bar{Z}^{n/}_{r_3,r_3} = \bar{Z}^n_{r_3,r_3} + Z_{ex,r3}$$

IV. Experimental Work and Results

A three-phase, four-pole wound rotor induction machine is utilized to evaluate the mathematical analysis. Data for this machine was given in Table I and some data was obtained from simulating the machine in CD-Adapco *SPEED* software.

It is not easy to obtain the impedance matrix using hand calculations, so it is reasonable for using MATLAB for calculations. The open circuit (running light test) and the short circuit (locked rotor test) were performed to obtain motor parameters. Based on these, an impedance parameter matrix is constructed. The windings coefficient turn ratio was 3.78, and this value is very close to measured one of 3.56. The magnetizing reactance and core losses were around the expected values.

The measurement of the rotor current and torque were taken with the rotor shorted circuited. Figs. 3, 4, and 5 illustrate the measured values of the torque and current against predicated values with neglecting harmonics components. It is sufficiently close to indicate the validity of the analysis. In the next test, a set of resistors will be used with two of the phases shorted and the remaining phase connected to a small resistor.

A loss of the steady torque and more oscillation will be introduced by an unbalanced rotor. This will be the subject of further work. Finally, voltages will be introduced to represent the inverter in a DFIG system.

TABLE I. MACHINE SPECIFICATION

Name plate details	
Power [HP]	10 (or 7.46 kW)
Speed [rpm]	1420
Frequency [Hz]	50
Stator voltage [V]	400/440 Delta
Stator rated current [A]	13
Rotor Voltage [V]	200
Rated rotor current [A]	22
Number of Poles	4
Slip [p.u.]	0.0533
Measured geometry [mm]	
Axial length rotor core	103.9
Axial length stator core	100.9
Stator outer diameter	353
Stator inner diameter	228.15
Rotor outer diameter	226.42
Shaft diameter	120
Airgap length	0.5
Stator slots	48
Stator slot opening	3.9
Turns per slot	34 in series
Stator wire diameter	1.725 – by calculation from *SPEED*
Stator winding	Single layer lap with 13 slot pitch
Coils per pole per phase	2
Stator slot depth	26.82
Stator tooth width	8.22
Rotor slot opening	3
Rotor slot depth	22.5
Slot width	3.5
Rotor wire diameter	1.9 mm from *SPEED*
Turns per coil	6 in series
Coils per phase	12
Rotor connection	Star through 3 slip rings
Measured resistances	
Rph stator (DC, cold)	1.82 ohm
Rph rotor (DC, cold)	0.23 ohm

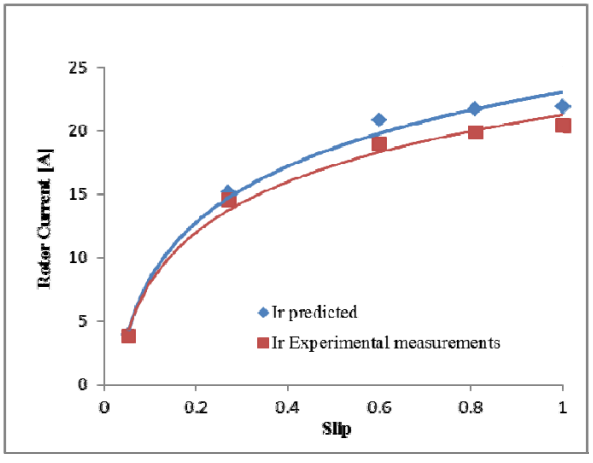

Fig. 3. Experimental and predicted currents versus slip for balanced rotor.

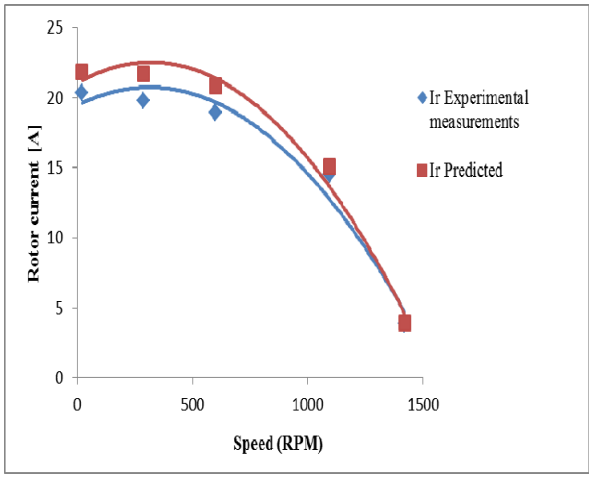

Fig. 4. Experimental and predicted currents versus speed characteristics for balanced rotor.

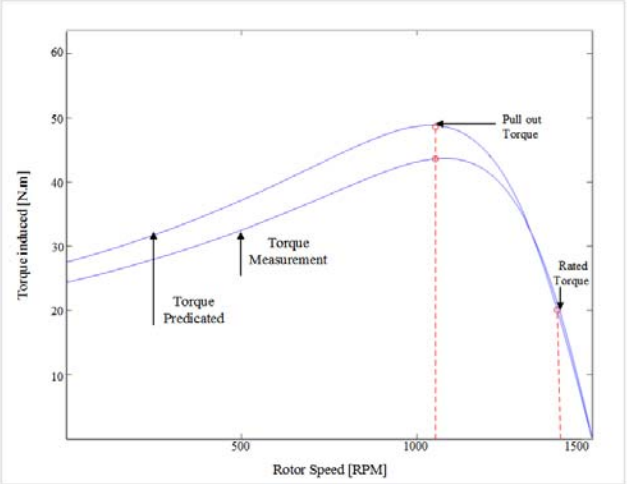

Fig. 5. Experimental and predicted torque versus speed characteristics for balanced rotor.

V. CONCLUSIONS

Impedance matrices that explain the behavior of the wound rotor motor are presented. Then the electromagnetic torque can be determined from stator and rotor current density distributions. The analysis can be used in two ways when dealing with a symmetrical and asymmetrical rotor, additionally it can be used to detect stator asymmetries reflecting into the rotor, this will be suggested for further research. The impedance matrix can be further developed in order to incorporate eccentricity faults and rotor winding or DFIG faults in wound rotor machines. These will be the subject of further study. However, as illustrated here, the impedance method is flexible and powerful and very suitable for use as the basis as a condition monitoring system.

ACKNOWLEDGMENT

The authors would like to sincerely thank Al-Hussein Bin Talal University for their financial support given through doctoral scholarship to the student Ahmad Salah.

REFERENCES

[1] M. Group, "Report of large motor reliability survey of industrial and commercial installations, Part II," *IEEE Trans. Ind. Appl*, vol. 21, pp. 865-872, 1985.

[2] EPRI, "Improved Motors for Utility Applications," *EPRI Final Report*, 1982.

[3] T. Barton and B. Doxey, "The operation of three-phase induction motors with unsymmetrical impedance in the secondary circuit," *Proceedings of the IEE-Part A: Power Engineering*, vol. 102, pp. 71-79, 1955.

[4] W. Ma and W. Leung, "Abnormal operation of induction motors with two-phase rotors," *International Journal of Electrical Engineering Education,* vol. 7, pp. 193-197, 1969.

[5] D. G. Dorrell, "*Calculation of unbalanced magnetic pull in cage induction machines*," Thesis, University of Cambridge, 1993.

[6] A. C. Smith, "Harmonic field analysis for slip-ring motors including general rotor asymmetry," *Industry Applications, IEEE Transactions on*, vol. 26, pp. 857-865, 1990.

[7] S. Williamson and M. Abdel-Magied, "Steady-state analysis of double-cage induction motors with rotor-cage faults," *in IEE Proceedings B (Electric Power Applications)*, 1987, pp. 199-206.

[8] S. Williamson and M. Mueller, "Calculation of the impedance of rotor cage end rings," *in IEE Proceedings B (Electric Power Applications)*, 1993, pp. 51-60.

[9] D. G. Dorrell, J. K. Shek, M. A. Mueller, and M.-F. Hsieh, "Damper windings in induction machines for reduction of unbalanced magnetic pull and bearing wear," *Industry Applications, IEEE Transactions on*, vol. 49, pp. 2206-2216, 2013.

[10] D. G. Dorrell, A. Salah, and O. Kayani, "The detection and suppression of unbalanced magnetic pull in wound rotor induction motors using pole-specific search coils and auxiliary windings," *Magnetics, IEEE Transactions on, 2015.*

[11] D. G. Dorrell and A. Salah, "Detection of rotor eccentricity in wound rotor induction machines using pole-specific search coils*," in Magnetics Conference (INTERMAG), 2015 IEEE*, 2015, pp. 1-1.

[12] S. Williamson and A. Smith, "Steady-state analysis of 3-phase cage motors with rotor-bar and end-ring faults," *in IEE Proceedings B (Electric Power Applications)*, 1982, pp. 93-100.